Pergamon

Cement and Concrete Research 31 (2001) 73–82

CEMENT AND CONCRETE RESEARCH

Review of the splitting-test standards from a fracture mechanics point of view

C. Rocco[a], G.V. Guinea[b,*], J. Planas[b], M. Elices[b]

[a]*Facultad de Ingeniería, Universidad Nacional de la Plata, La Plata, Argentina*
[b]*Departamento de Ciencia de Materiales, Universidad Politécnica de Madrid, Madrid, Spain*

Received 3 March 2000; accepted 5 September 2000

Abstract

This article analyzes by means of fracture mechanics the current splitting-test standards for concrete. The cohesive crack model, which has shown its utility in modeling the fracture of concrete and other cementitious materials, has been used to assess the effect of the specimen size, the specimen shape and the width of the load-bearing strips on the conventional splitting tensile strength, f_{st}. The results show that, within the ranges recommended in the standards, the values of the splitting tensile strength can differ by up to 40%, and, consequently, f_{st} can hardly be assumed to be a material property. Empirical formulae for concretes with different compressive strength (10–80 MPa) and maximum aggregate size (8–32 mm) have been used to show that f_{st} is nearly specimen independent only for certain compositions, such as high-strength concretes, or when the aggregate size is under 16 mm. New closed-form expressions for f_{st} are given in this paper to incorporate the effect of material properties, and some recommendations are drawn to minimize the influence of the width of the load-bearing strips.

Keywords: Tensile properties; Fracture; Concrete; Modeling

1. Introduction

The splitting tensile test is used worldwide to measure the tensile strength of concrete. This test was first proposed by Lobo Carneiro and Barcellos during the Fifth Conference of the Brazilian Association for Standardization in 1943 [1], hence, its other denomination — the Brazilian test; now, it is a standardized test method included in the major international concrete standards such as ASTM C-496, ISO 4105, BS 1881-117 and others [2–4].

The main advantage of the splitting test is that only external compressive loads are required. A cylindrical or prismatic specimen is compressed along two diametrically opposed generators so that a nearly uniform tensile stress is induced in the loading plane. To prevent local failure in compression at the loading generators, two thin strips, usually made of plywood, are placed between the loading platens and the specimen to distribute the load. The induced tensile stress state causes the specimen to fail by splitting. The maximum value of the tensile stress, computed at failure from the theory of elasticity, is the splitting tensile strength, f_{st}, ordinarily assumed in the standards to be a material property.

It is important to note that specimens of different geometry, size and width of the load-bearing strips are prescribed in the various standards, whereas the splitting tensile strength is computed with a single formula that does not take account of these variables. The effect of the geometry and the width of the load-bearing strips have been analyzed theoretically since the early day of splitting test application [5–8], usually within the framework of the classical theory of elasticity. These works have shown that when the specimen types and the load-bearing strips recommended in the standards are used, the splitting strength determined via the standard equation only varies by 4%.

A more refined analysis of the splitting test by the authors based on the cohesive crack model [9] has demonstrated that the results from the classical theory of elasticity are not applicable to cementitious materials such as mortar or concrete. From this analysis, it has been shown that the standardized f_{st} can vary significantly with the specimen

* Corresponding author. Departamento de Ciencia de Materiales, ETSI Caminos, Ciudad Universitaria s/n, 28040 Madrid, Spain. Tel.: +34-9-1-336-6754; fax: +34-9-1-336-6680.

E-mail address: gguinea@mater.upm.es (G.V. Guinea).

0008-8846/01/$ – see front matter
PII: S0008-8846(00)00425-7

geometry, the width of load-bearing strips and the specimen size. The main consequence is that the specimen type and the width of the load-bearing strips prescribed in the standards can influence the computed value of the conventional splitting tensile strength by as much as 40%. This has been experimentally corroborated by the authors testing granite and concrete specimens [10].

This article reviews the current standards on splitting tensile testing from a fracture mechanics point of view by means of the cohesive crack model. The results are compared with the classic linear-elastic approach, discussing the limitations of this theory. The influence of both the specimen geometry and the width of the load-bearing strips is analyzed within the context of various standards, and new closed-form expressions for f_{st} are given to incorporate the effect of material properties. Finally, some recommendations are drawn to minimize the influence of the load-bearing strips on the measurement.

2. The splitting test

2.1. Description of the test

In the splitting (or Brazilian) test, a cylindrical or prismatic specimen is compressed along two diametrically opposed generators as shown schematically in Fig. 1. To prevent multiple cracking and crushing at the points of loading, the load is distributed through two bearing strips whose width, b, differs in the various standards. If the material behaviour is linear-elastic, this geometry leads to a nearly uniform tensile stress along the plane of loading, and the expected rupture mode is the splitting of the specimen in two halves across that plane. In the case of concentrated loads, the maximum tensile stress on this plane can be calculated by [11]:

$$\sigma_{\max,P} = \frac{2P}{\pi BD} \tag{1}$$

where $\sigma_{\max,P}$ is the maximum tensile stress in the specimen

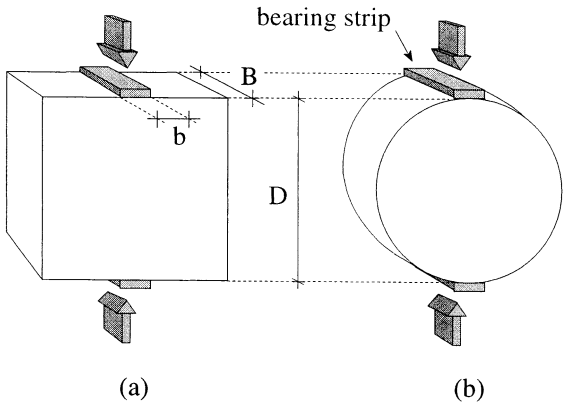

Fig. 1. Cylindrical and cubical specimens.

Table 1
Standard specimens for the Brazilian test

Standard	Specimen				Bearing strip (b (mm))
	Notation	Type	D (mm)	B (mm)	
ASTM C496	ASTM150/16	cylindrical	150	300	25
BS 1881-117	BS_c150/10	cylindrical	150	300	15±2
BS 1881-117	BS_q100/4	cubical	100	100	4±1
BS 1881-117	BS_q100/15	cubical	100	100	15±2
BS 1881-117	BS_q150/4	cubical	150	150	6±1
BS 1881-117	BS_q150/10	cubical	150	150	15±2

when the applied load is P,D and B are the specimen depth and thickness, respectively (Fig. 1).

Following the standards, the maximum tensile stress at failure — calculated from the theory of elasticity — is a material property called splitting tensile strength, f_{st}. If the load-bearing strips are narrow enough to consider the loading concentrated, and the material behaviour is linear-elastic–brittle, f_{st} is close to the tensile strength determined by an ideal uniaxial tensile test.

From Eq. (1), the splitting tensile strength f_{st} is evaluated in the standards by:

$$f_{st} = \frac{2P_u}{\pi BD} \tag{2}$$

where P_u is the maximum load recorded during the test. The splitting tensile strength is then calculated on the assumption of a hypothetical load-bearing strip of zero width (concentrated load).

2.2. Standards

The splitting test is incorporated into all major concrete standards and into many design codes for concrete structures such as ACI-318R [12] and CEB-90 [13]. In all of them, the testing procedure is the same, but some differences emerge regarding the specimen geometry, the specimen size and the width of the load-bearing strips. Table 1 shows the values recommended by two standards usually taken as a reference: ASTM C496 and BS 1881-117. As shown in the table, very different combinations of specimen geometry (cube or cylinder), specimen size (100 and 150 mm) and relative width of the load-bearing strips ($b/D = 0.04–0.16$) can be used in the tests. However, the evaluation of the splitting tensile strength, f_{st}, is always made through Eq. (2), independent of these parameters. The consequences of this assumption will be examined in the following sections.

3. Review of the linear-elastic solution

As already mentioned, the standard equation to calculate the splitting tensile strength is derived from elasticity theory assuming that two compressive line loads are applied in two

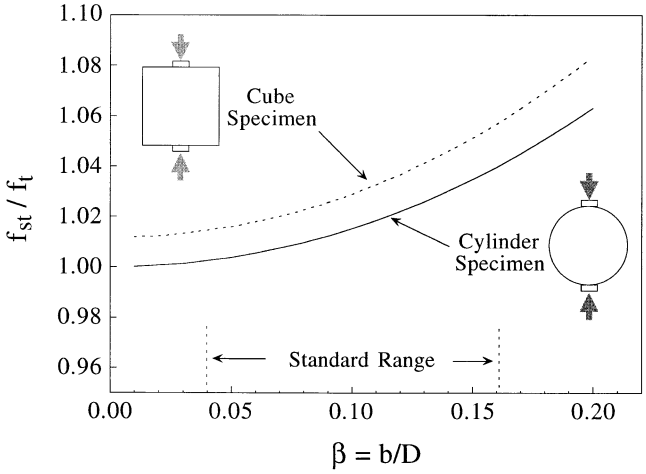

Fig. 2. Variation of the splitting tensile strength with the relative width of the load bearing strips according to the theory of elasticity.

opposite sides of the specimen; i.e. the load is distributed along a line of zero width. However, this assumption is violated in the standards since bearing strips of finite width are prescribed to distribute the load and, consequently, the tensile stress distribution from which Eq. (2) was derived is not fulfilled in practice. As the width of the load-bearing strips increases, the maximum value of the tensile stress along the plane of loading decreases, for any given value of the load. Then, the splitting tensile strength calculated from Eq. (2) is overestimated.

For cylindrical and cubical specimens, the dependence of the maximum tensile stress at the plane of loading on the width of the load-bearing strips can be calculated from [14]:

$$\sigma_{max} = \frac{2P}{\pi BD}(1-\beta^2)^{3/2} \qquad \text{for cylindrical specimens} \tag{3a}$$

$$\sigma_{max} = \frac{2P}{\pi BD}[(1-\beta^2)^{5/3} - 0.0115] \quad \text{for cubical specimens} \tag{3b}$$

where B and D are the specimen dimensions (see Fig. 1), P is the load, and $\beta = b/D$ is the relative width of the load-bearing strips. Both equations are valid for $\beta \leq 0.20$.

In brittle materials with linear-elastic behavior, it is generally assumed that failure occurs when the maximum tensile stress reaches a critical value. If, for practical purposes, we assume that this critical value coincides with the true tensile strength, f_t — obtained from an ideal uniaxial test — the failure criterion can be written from Eqs. (3a) and (3b) as:

$$f_t = \frac{2P_u}{\pi BD}(1-\beta^2)^{3/2} \qquad \text{for cylindrical specimens} \tag{4a}$$

$$f_t = \frac{2P_u}{\pi BD}[(1-\beta^2)^{5/3} - 0.0115] \quad \text{for cubical specimens} \tag{4b}$$

where P_u is the maximum load recorded during the test (the peak load). Note that by definition f_t coincides with the theoretical value of the splitting tensile strength for a cylindrical specimen with $b/D = 0$.

The splitting tensile strength evaluated from the standard test is given by Eq. (2), and by taking into account Eqs. (4a) and (4b), it can be rewritten as:

$$f_{st,c} = f_t(1-\beta^2)^{-3/2} \qquad \text{for cylindrical specimens} \tag{5a}$$

$$f_{st,q} = f_t[(1-\beta^2)^{5/3} - 0.0115]^{-1} \qquad \text{for cubical specimens} \tag{5b}$$

where $f_{st,c}$ and $f_{st,q}$ refer to the splitting tensile strength for cylinders and cubes, respectively.

Fig. 2 shows the splitting tensile strength in terms of the tensile strength f_t as a function of the relative width of the load-bearing strips β [Eqs. (5a) and (5b)]. According to this theoretical prediction, the splitting tensile strength increases with the width of the load-bearing strips. Nevertheless, within the range prescribed by the standards ($0.04 \leq \beta \leq 0.16$), the differences with f_t are within a 6% deviation, which corresponds to the larger width permitted in the standards — $\beta = 0.16$ — and when f_{st} is evaluated from cubical specimens.

The effect of specimen geometry can be analyzed by comparing Eqs. (5a) and (5b). The ratio between the splitting strengths of cubes and cylinders is:

$$\frac{f_{st,q}}{f_{st,c}} = \frac{(1-\beta^2)^{3/2}}{(1-\beta^2)^{5/3} - 0.0115} \tag{6}$$

Fig. 3 plots Eq. (6). The differences between the two splitting strengths are not noticeable — well under 2% for the standard range — although for a given value of the relative width, β, the splitting strength for cubes is always higher.

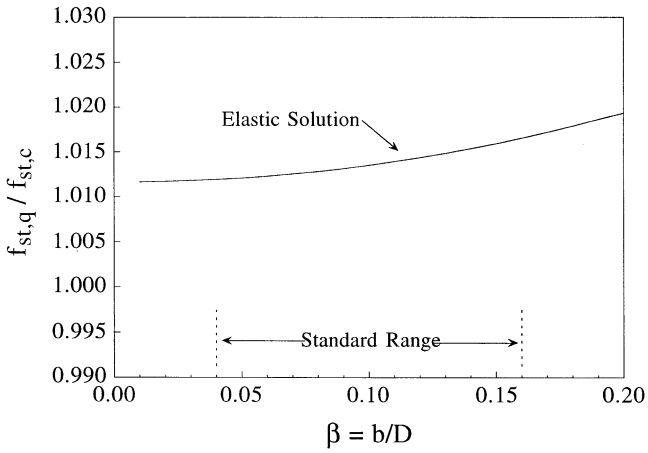

Fig. 3. Variation of the relation between cube and cylinder splitting tensile strength with the relative width of the load bearing strips according to the theory of elasticity.

These results justify the use in the standards of a very simple equation such as Eq. (2) to estimate the splitting tensile strength. Within the framework of the theory of elasticity, and assuming a purely brittle material, the error due to applying this equation, which does not take into account either the specimen geometry or the width of the load-bearing strips, is under 6%. Experimental results shown in the following section will demonstrate that this is not always the case when testing concrete specimens, and that a more refined analysis based on fracture mechanics concepts is required.

4. Fracture mechanics approach

The analysis shown in the preceding section was made for perfectly brittle materials with linear-elastic behavior. Unfortunately, this is not the case of the so-called quasi-brittle materials such as concrete, rock and ceramics, in which the growth and coalescence of initial flaws before the peak load causes a nonlinear behavior. The most significant consequence of this non linearity is the phenomenon known as size effect, which cannot be explained by the classical rupture criterion of limit analysis theory [15]. A more detailed analysis by the cohesive crack model — which has shown its utility in modeling the fracture of concrete and other cementitious materials [16] — is presented in this section. With this model, the size effect in the splitting test is numerically analyzed and the results are compared to the elastic solution.

4.1. The cohesive crack model

In this model, it is assumed that as soon as the tensile strength f_t is reached at any point in the material, a crack perpendicular to the maximum stress direction is produced. This crack is not immediately stress free, but still transfers stress while opening as shown in Fig. 4.

In a simple implementation of the model, the following hypotheses can be assumed: (1) the bulk material can be approximated by an isotropic linear-elastic material with elastic modulus E and Poisson coefficient ν, and (2) the analysis is restricted to pure crack opening and to monotonic loading. Then, the stress σ transferred at any point of the crack is related univocally to the crack opening w at this point. The function relating σ and w is called the softening curve, and is assumed to be a material property (Fig. 4).

For unnotched specimens — as those used in the Brazilian test — only the initial portion of the softening curve is relevant if the analysis is restricted to the determination of stresses and displacements up to the maximum load [17]. Then, an initial linear approximation of the softening curve defined by the tensile strength f_t and the horizontal intercept of the initial slope w_1 can be used instead of the complete curve (see Fig. 4), and the material properties f_t and w_1,

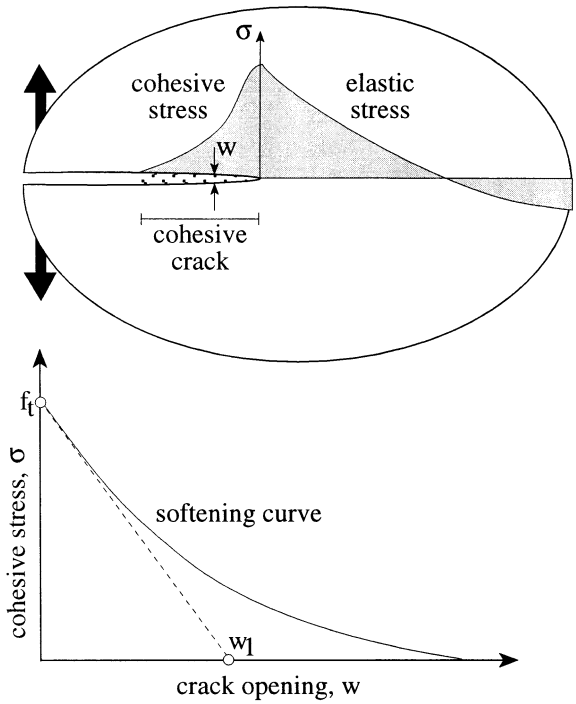

Fig. 4. Cohesive crack and softening curve.

together with the elastic modulus E, suffice to determine the peak load. Based on dimensional grounds, it can be shown that it is not the size of the specimen itself, D, that influences the peak load but the size relative to a parameter called the reduced characteristic length, l_{ch1}, defined as [18]:

$$l_{ch1} = \frac{Ew_1}{2f_t} \tag{7}$$

The value of l_{ch1} for concrete is usually in the range 50–400 mm. Typical values of l_{ch1} for different concrete strengths and aggregate sizes — estimated from empirical formulas recommended in the CEB Code Model — are given in Appendix A.

4.2. Splitting strength and size effect

The size effect on the splitting strength has been experimentally and numerically analyzed by the authors by means of the cohesive crack model [9,10]. From this work, the following analytical expression to estimate the size effect on the splitting tensile strength is proposed:

$$f_{st} = \frac{f_t}{c_1 + c_2(D/l_{ch1})} + c_3 f_t \tag{8}$$

where f_t is the tensile strength — obtained from an ideal uniaxial tensile test, D the specimen size according to Fig. 1, l_{ch1} the reduced characteristic length given by Eq. (7) and c_1, c_2 and c_3 are coefficients depending on both the specimen geometry and the width of the load-bearing strips. Table 2 shows some values of these coefficients for cylindrical and cubical specimens.

Table 2
Coefficients c_i to Eq. (8) for cylindrical and cubical specimens

	Cylindrical specimen			Cubical specimen		
b/D	c_1	c_2	c_3	c_1	c_2	c_3
0.02	− 215.36	921.61	1.0004	27.412	17.799	1.0046
0.04	− 100.84	370.6	1.0013	2.348	49.741	1.0111
0.06	− 49.903	182.83	1.0018	− 12.291	60.940	1.0157
0.08	− 29.714	108.19	1.0032	− 12.534	50.200	1.0198
0.10	− 19.302	70.614	1.0066	− 10.142	38.633	1.0246
0.12	− 13.301	49.275	1.0112	− 7.813	29.624	1.0304
0.14	− 9.567	36.040	1.0169	− 6.119	23.347	1.0373
0.16	− 7.215	27.534	1.0238	− 4.888	18.873	1.0456
0.18	− 5.544	21.526	1.0318	− 3.891	15.401	1.0550

Fig. 5a and b shows the predictions of the splitting tensile strength by the cohesive crack model — Eq. (8) — for some experimental results obtained from granite and concrete specimens. The theoretical predictions for both granite cylindrical and concrete prismatic specimens are very good. As shown in these figures, the cohesive crack model captures well the size effect and the influence of the width of the load-bearing strips. Details of the experiments can be found in Ref. [10].

To compare the solutions for elastic–brittle — Eqs. (5a) and (5b) — and cohesive fracture behaviour, f_{st} is plotted in Fig. 6a and b as a function of the width of the load-bearing strips, b/D, for several relative specimen sizes, D/l_{ch1}. Fig. 6a and b also shows the predictions based on the theory of elasticity. For a given material, i.e. for a given value of f_t and l_{ch1}, the prediction based on fracture mechanics shows that f_{st} is strongly dependent on both variables. On modifying the specimen size or the width of the load-bearing strips the evaluated splitting tensile strength can vary by as much as 40%, much greater than can be justified from the theory of elasticity. Only for very large specimens ($D/l_{ch1} \approx 3$) do the results from the theory of elasticity and from fracture mechanics come together. As an example, if $l_{ch1} = 150$ mm is a usual figure for an ordinary concrete, diameters of the order of half a meter would be required to approximate the brittle–elastic limit.

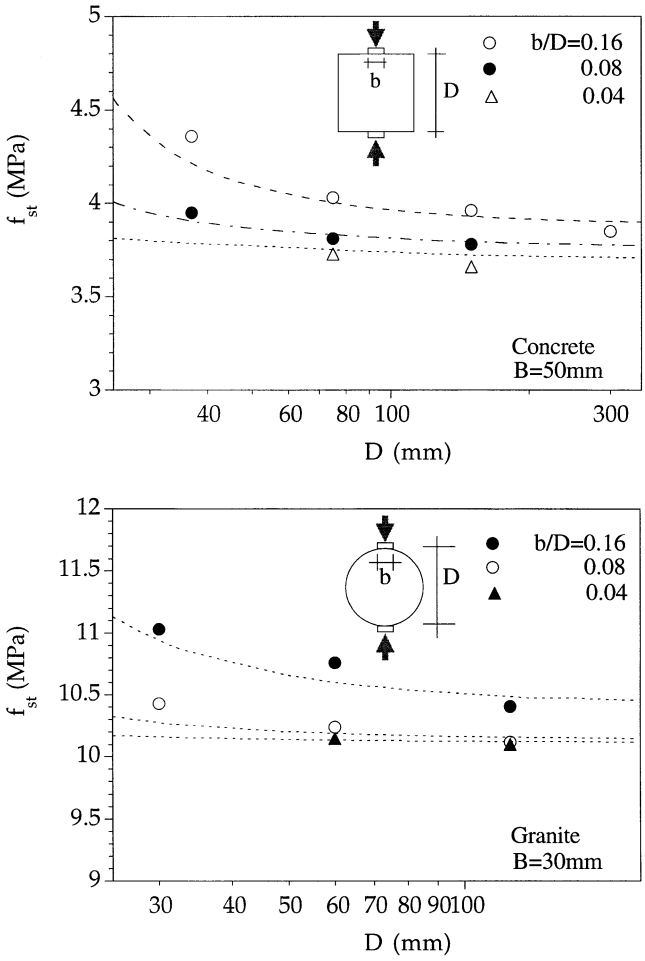

Fig. 5. (a) Prediction of the splitting tensile strength with the cohesive crack model. Granite cylindrical specimens. (b) Prediction of the splitting tensile strength with the cohesive crack model. Concrete cubical specimens.

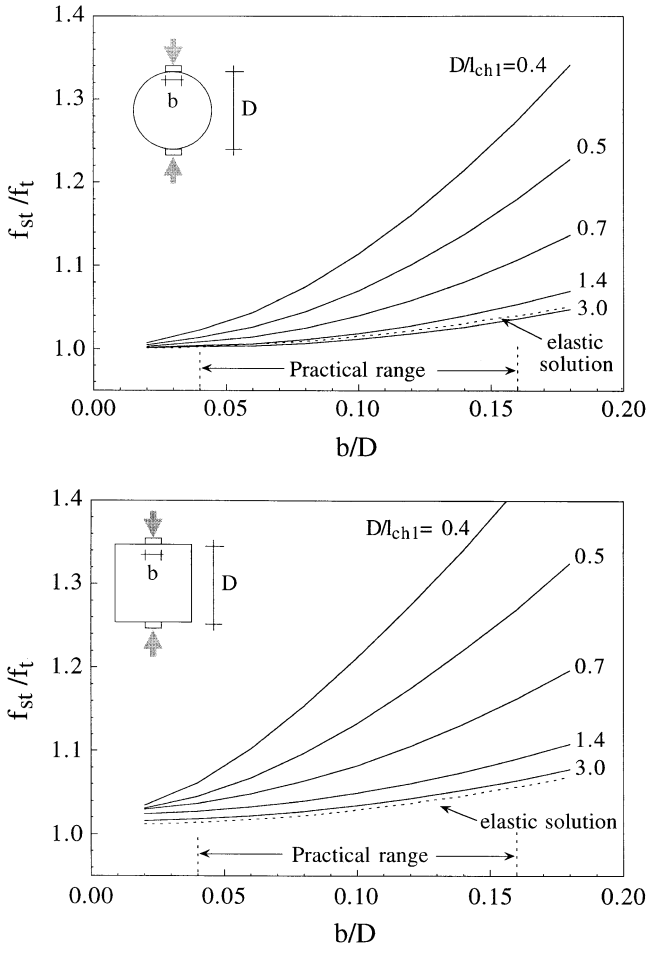

Fig. 6. (a) Variation of the splitting tensile strength with the relative width of the load-bearing strips according to the cohesive crack model, cylindrical specimens. (b) Variation of the splitting tensile strength with the relative width of the load-bearing strips according to the cohesive crack model, cubical specimens.

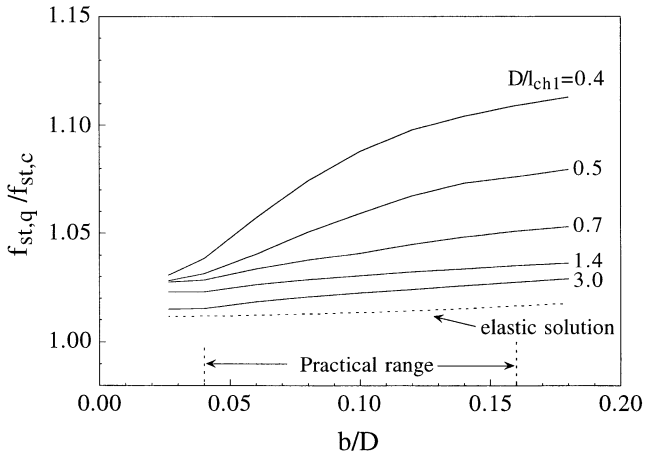

Fig. 7. Ratio of cube to cylinder splitting tensile strength as a function of the relative width of the load-bearing strips according to the cohesive crack model.

Due to the size effect, the splitting tensile strength cannot be accepted as a material property. However, the results show that when the width of the load-bearing strips approaches zero, the size effect vanishes and a nearly constant value of f_{st} — which approximates the tensile strength, f_t — can be obtained.

Fig. 7 shows the influence of the geometry on f_{st}. In this figure, the ratio between the splitting strength of cubical and cylindrical specimens obtained from Eq. (8), $f_{st,q}/f_{st,c}$, is plotted as a function of both the specimen size and the width of load-bearing strips. As a reference, the predictions based on the theory of elasticity, Eq. (6), are also plotted. Note that even for specimens of identical size and width of the load-bearing strips, the splitting tensile strength evaluated from cubes and cylinders can differ by up to 12%. Again, this difference is much greater than can be justified from the theory of elasticity.

Results in Figs. 6a,b and 7, clearly show that if the influence of both the load-bearing strips and the specimen geometry (shape and size) are not taken into account, as in the standard formula, Eq. (2), noticeable errors in the estimation of the splitting tensile strength arise, making the standardized splitting tensile strength a non-homogeneous value.

5. Application to standard specimens

When the specimen size and the width of the load-bearing strips prescribed in each standard (Table 1) are incorporated into Eq. (8), the following particular expressions for the splitting tensile strength are obtained:

$$f_{st} = \frac{f_t}{-7.215 + 4130/l_{ch1}} + 1.0238 f_t \qquad \text{ASTM} - 150/16 \tag{9a}$$

$$f_{st} = \frac{f_t}{-19.302 + 10592/l_{ch1}} + 1.0066 f_t \qquad \text{BS}_c - 150/10 \tag{9b}$$

$$f_{st} = \frac{f_t}{-10.142 + 5795/l_{ch1}} + 1.0246 f_t \qquad \text{BS}_q - 150/10 \tag{9c}$$

$$f_{st} = \frac{f_t}{2.348 + 7461/l_{ch1}} + 1.0111 f_t \qquad \text{BS}_q - 150/4 \tag{9d}$$

$$f_{st} = \frac{f_t}{-5.491 + 2099/l_{ch1}} + 1.0414 f_t \qquad \text{BS}_q - 100/15 \tag{9e}$$

$$f_{st} = \frac{f_t}{2.348 + 4974/l_{ch1}} + 1.0111 f_t \qquad \text{BS}_q - 100/4 \tag{9f}$$

where the reduced characteristic length, l_{ch1}, is introduced in millimeters. For ASTM C496 and BS1881-117 test standards, these equations give the variation of the splitting tensile strength with the material properties f_t and l_{ch1}, as predicted by the cohesive crack model.

Fig. 8 plots the dependence of f_{st} on l_{ch1} according to Eqs. (9a)–(9f). To compare the results, the values of f_{st} have been referenced to that of ASTM C496 cylinder ($D = 150$ mm, $L = 300$ mm, $b/D = 0.16$), which is adopted as the reference value. The variation range predicted by the theory of elasticity is also displayed in the same figure as a grey band. The curves show that, except for the $BS_q100/15$ specimen, the ASTM C496 standard delivers a value of the splitting tensile strength larger than that of the British Standard. These results, based on the cohesive crack model, show that f_{st} can differ by up to 30% from one standard to another depending on the material properties, a difference much greater than expected when the analysis is based on the theory of elasticity. On the other hand, for reduced l_{ch1} values — which correspond to brittle materials — the differences vanish, and all the splitting tensile strengths converge to f_t, the ideal uniaxial tensile strength.

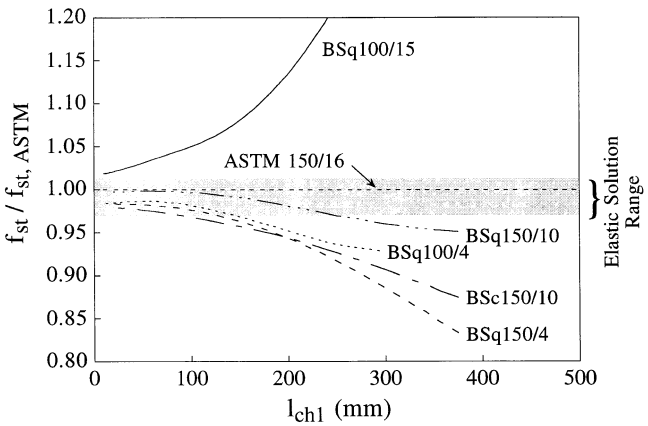

Fig. 8. Relative splitting tensile strength from various standard specimens according to cohesive crack model predictions.

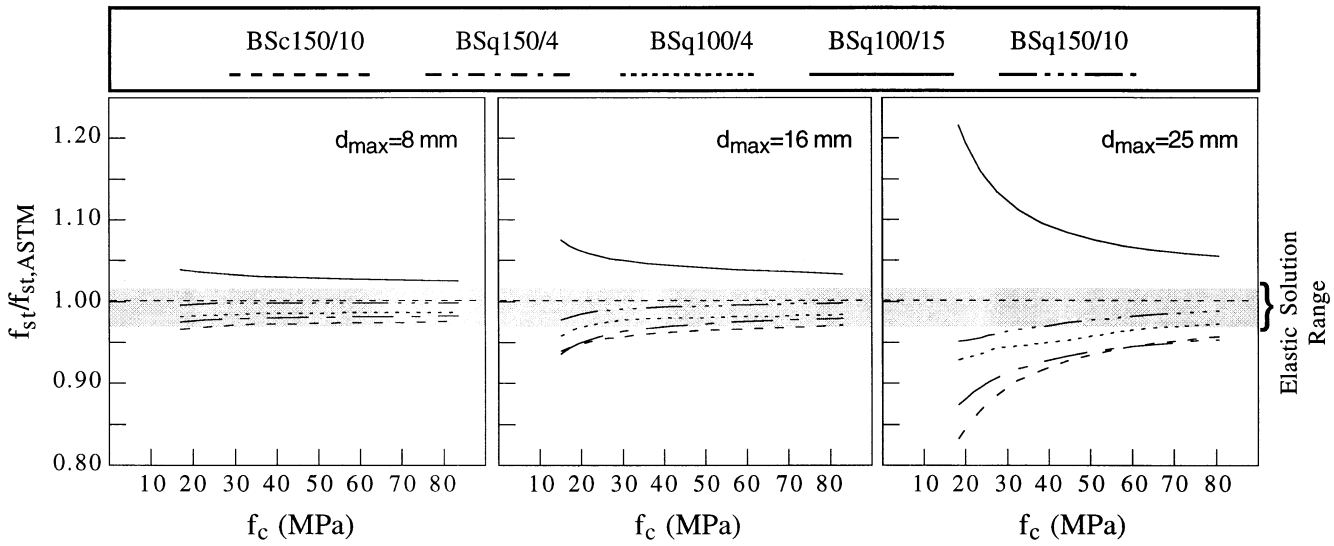

Fig. 9. Empirical variation of the splitting tensile strength for various concrete standard specimens as a function of the compressive strength and the maximum aggregate size.

Eqs. (9a)–(9f) can help in converting splitting tensile strengths from BS to ASTM standards, although this conversion is not simple because the reduced characteristic length l_{ch1} has to be known. For practical purposes, l_{ch1} can be empirically inferred from the compressive strength, f_c, and the maximum aggregate size, d_{max}, two parameters commonly available for any concrete. The relationship is developed in Appendix A, where l_{ch1} is estimated from the bilinear softening curve recommended in the CEB-90 Model Code (Fig. 12a). The results of this analysis are plotted in Fig. 12b in Appendix A, and have been used to produce Fig. 9, which shows the variation of the splitting tensile strength as a function of the compressive strength and the maximum aggregate size. Again, as displayed in this figure, ASTM and BS test standards can differ by up to 30% in f_{st} within the practical interest range, but the differences fall to acceptable limits if high strength concretes or concretes with small size aggregates are considered.

6. Relation between the splitting strength and the "true" tensile strength

It is a common practice in concrete standards to give empirical equations relating the compressive strength to other mechanical properties such as the modulus of rupture, the splitting tensile strength or the uniaxial tensile strength, from which it is possible to correlate the splitting tensile strength and the uniaxial tensile strength. Sometimes, an explicit equation for these two variables is supplied, as in the CEB-90 Model Code that gives the following relationship:

$$f_t = 0.90 f_{st} \tag{10}$$

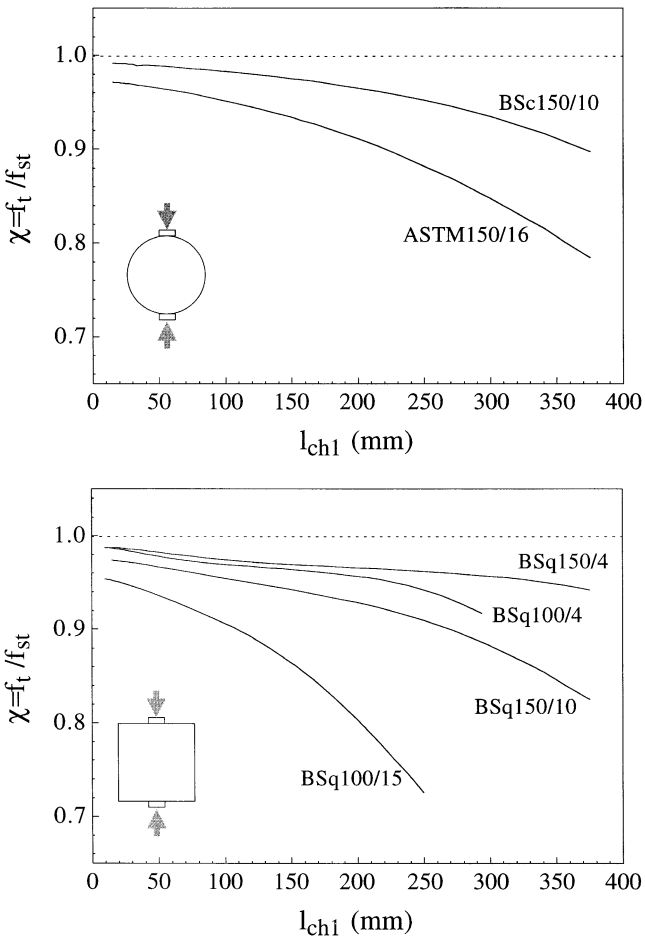

Fig. 10. (a) Ratio of tensile strength to splitting tensile strength for cylindrical standard specimens according to cohesive crack model predictions. (b) Ratio of tensile strength to splitting tensile strength for cubical standard specimens according to cohesive crack model predictions.

independent of the material properties, and, consequently, in opposition to the fracture mechanics approach presented in Eqs. (9a)–(9f), where, depending on the material properties — condensed in the parameter l_{ch1} — the relation between the tensile strength and the splitting tensile strength can vary considerably. This is shown graphically in Fig. 10a and b, where the f_t/f_{st} ratio obtained from these equations is plotted vs. the reduced characteristic length, l_{ch1}. Depending on both the specimen and the material properties, f_t/f_{st} can vary by up to 35%, and only the specimens with small b/D such as $BS_q150/4$ and $BS_q100/4$ show a nearly constant ratio.

These results suggest that material-independent correlation formulas such as Eq. (10), are suitable only within a very narrow range. Fig. 11a compares the prediction of f_t/f_{st} by the cohesive crack model for the standard ASTM specimen, Eq. (9a), with the CEB-90 reference value, which shows that for l_{ch1} larger than 220 mm the reference value overestimates the tensile strength.

The influence of the concrete properties on the f_t/f_{st} ratio can be analyzed in a better way if the empirical dependence

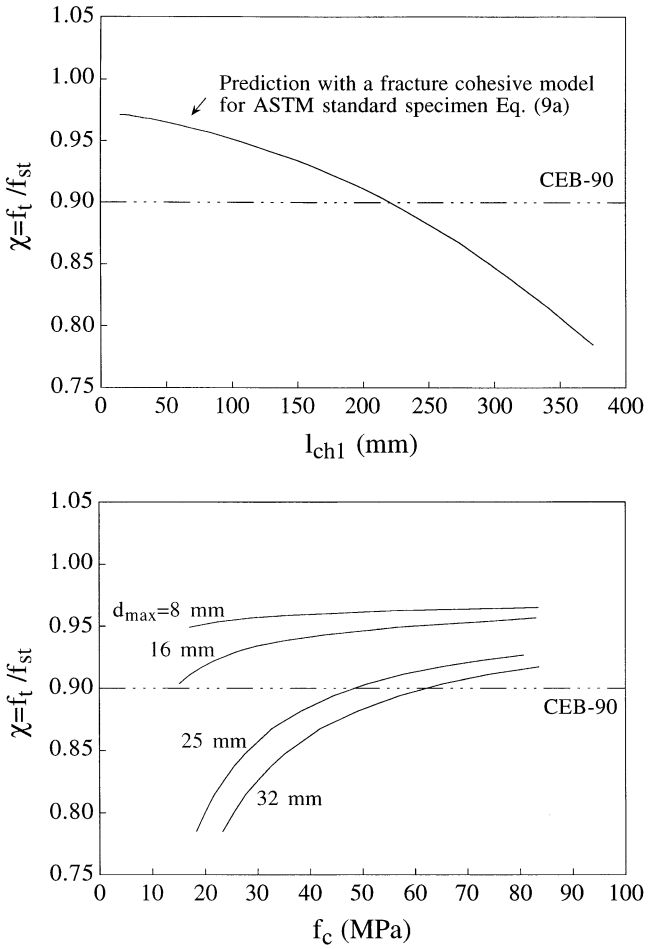

Fig. 11. (a) Ratio of the tensile strength to the splitting tensile strength. Comparison of the cohesive crack model to CEB standard proposal. (b) Empirical variation of the ratio f_t/f_{st} with the compressive strength and the maximum aggregate size.

of l_{ch1} on the compressive strength and on the maximum aggregate size derived in Appendix A is taken into account. Then the curves plotted in Fig. 11b are obtained, which shows that for ordinary concretes with compressive strengths between 20 and 40 MPa and aggregate size larger than 16 mm, the CEB standard systematically overestimates the tensile strength f_t. Conversely, when high-strength concretes are considered, this standard is on the conservative side.

7. Conclusions

Both the specimen geometry and the width of the load-bearing strips are variables systematically neglected in the standards when evaluating the splitting tensile strength of concrete. Consequently, the values of f_{st} from different standard specimens can differ significantly. A fracture mechanics approach based on the cohesive crack model shows that the difference can be as high as 30% from one standard to another. Given this dependence, the standardized splitting tensile strength should not be considered a material property. The results show that the differences become smaller as the material tested becomes more brittle, although in ordinary strength concrete, the differences may be noticeable.

With the cohesive crack mode some closed-form analytical expressions for the tensile splitting strength were obtained for the standard specimens. In these equations, f_{st} is given as a function of the material properties E, f_t and G_F. The proposed expressions can help to compare the splitting strength evaluated from different standard specimens.

The dependence of f_{st} on the specimen geometry and on the width of the load-bearing strips concerns the relation between the splitting tensile strength and the uniaxial tensile strength f_t. By using the proposed expressions for f_{st}, the f_{st}/f_t ratio is seen to vary by 1.03–1.35, and the difference increases as the load-bearing strips become wider. From this point of view, the load-bearing strips recommended in the ASTM standard seem to be too wide. A relative width closer to 4% appears to be sound.

Acknowledgments

The authors gratefully acknowledge support for this research provided by CICYT, Spain, under grants MAT-97-1022 and MAT-97-1007-C02-02, and by the Ministerio de Educación y Ciencia, Spain, through the Foreign Researchers Program.

Appendix A.

A.1. CEB-90 model code softening curve

In the CEB-90 Model Code, the bilinear softening curve shown in Fig. 12a is recommended for ordinary concrete,

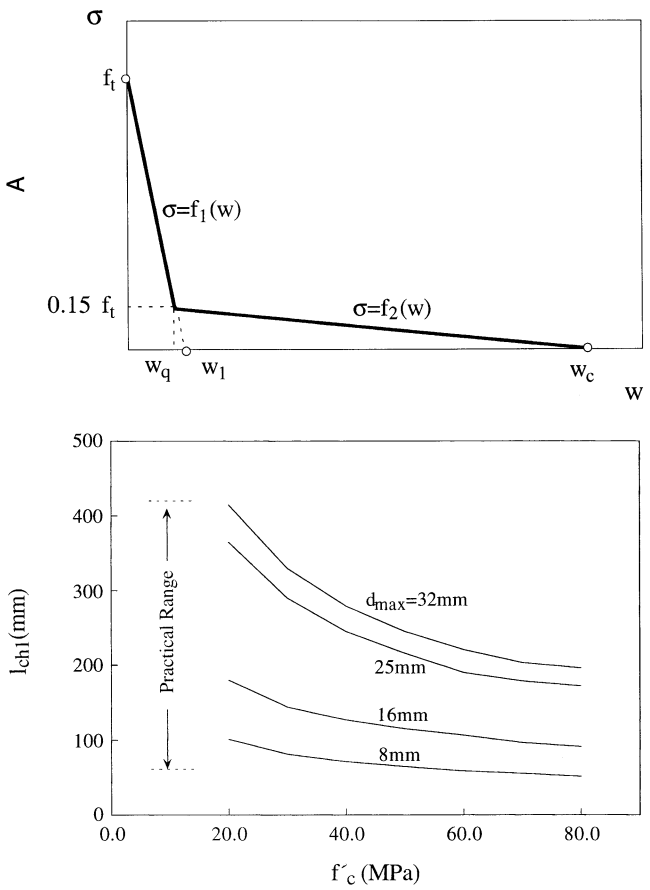

Fig. 12. (a) Bilinear softening curve recommended in the CEB-90 Model Code. (b) Empirical relation between l_{ch1}, f_c and d_{max} derived from the CEB Model Code estimations.

where the analytical expressions for the bilinear curve are [Eqs. (a.1) and (a.2)]:

$$\sigma = f_t(1 - 0.85w/w_1) \qquad \text{for } 0 \le w \le w_q \tag{a.1}$$

$$\sigma = \frac{0.15f_t}{w_c - w_1}(w_c - w_1) \qquad \text{for } w_q \le w \le w_c \tag{a.2}$$

with Eqs. (a.3) and (a.4) expressed as:

$$w_q = \frac{G_F}{f_t}(2 - 0.15\beta_F) \tag{a.3}$$

$$w_c = \frac{G_F}{f_t}\beta_F \tag{a.4}$$

and the coefficient β_F depends on the maximum aggregate size. In the CEB Model Code values of β_F equal to 8, 7 and 5 are recommended for maximum aggregate sizes of 8, 16 and 32 mm, respectively.

From Eqs. (a.1) and (a.3), the following expression for w_1, the horizontal intercept of the initial tangent, can be derived:

$$w_1 = 1.176\frac{G_F}{f_t}(2 - 0.15\beta_F) \tag{a.5}$$

A.2. Empirical values for l_{ch1}

In Eq. (6), the parameter l_{ch1} was defined as:

$$l_{ch1} = \frac{Ew_1}{2f_t} \tag{a.6}$$

For practical purposes, w_1 can be estimated using Eq. (a.5), which was obtained from the bilinear softening curve recommended in the CEB-90 Model Code. Then, substituting Eq. (a.5) in Eq. (a.6), l_{ch1} is obtained as [Eq. (a.7)]:

$$l_{ch1} = 0.588(2 - 0.15\beta_F)\frac{EG_F}{f_t^2} \tag{a.7}$$

where G_F, E and f_t can be estimated in a coarse approximation by using the empirical values supplied in the Model Code. With this approximation, only the compressive strength f_c and the maximum aggregate size d_{max} are required. Fig. 12b shows the result: An empirical relationship between l_{ch1}, f_c and d_{max}. In this figure, the values for $d_{max} = 25$ mm — not given in the CEB Model Code — have been obtained by interpolation.

References

[1] F. Lobo Carneiro, A. Barcellos, Résistance a la Traction des Bétons, Int. Assoc. Test. Res. Lab. Mater. Struct. RILEM Bull. 13 (1949) 98–125.
[2] ASTM C496-90, Standard test method for splitting tensile strength of cylindrical concrete specimens, Annu. Book ASTM Stand. 4 (04.02) (1991) 266–269.
[3] BS 1881: Part 117, Testing concrete method for the determination of tensile splitting strength, Br. Stand. Inst. (1983).
[4] ISO 4108-1980 (E), Concrete determination of tensile splitting strength of test specimen, Int. Stand. (1980).
[5] P. Wright, Comments on an indirect tensile test on concrete cylinders, Mag. Concr. Res. 20 (1955) 67–79 (July).
[6] T. Tang, Effects of load-distributed width on split tension of unnotched and notched cylindrical specimens, J. Test. Eval. 22 (5) (1994) 401–409.
[7] J. Davies, D. Bose, Stress distribution in splitting test, ACI J. 65 (1968) 662–669.
[8] H. Petroski, R. Ojdrovic, The concrete cylinder: Stress analysis and failure modes, Int. J. Fract. 34 (1987) 263–279.
[9] C. Rocco, G.V. Guinea, J. Planas, M. Elices, Size effect and boundary condition in the Brazilian tests: Theoretical analysis, Mater. Struct. 32 (1999) 437–444.
[10] C. Rocco, G.V. Guinea, J. Planas, M. Elices, Size effect and boundary condition in the Brazilian tests: Experimental verification, Mater. Struct. 32 (1999) 210–217.
[11] S.P. Timoshenko, J.N. Goodier, Theory of Elasticity, McGraw-Hill, New York, 1991.
[12] ACI-318R, ACI manual of concrete practice, Am. Concr. Inst. (1993).
[13] CEB-90, Final draft CEB-FIP model code 1990, Bull. Inf. Com. Euro-Int. Beton 203 (1991).
[14] C. Rocco, G.V. Guinea, J. Planas, M. Elices, The effect of the boundary conditions on the cylinder splitting strength, in: F.H. Wittmann (Ed.), Fracture Mechanics of Concrete Structures, Proceedings FRAMCOS-2, Aedificatio Publishers, Freiburg, 1995, pp. 75–84.

[15] J. Planas, M. Elices, Size effect in concrete structures: Mathematical approximations and experimental validation, in: J. Mazars, Z.P. Bazant (Eds.), Cracking and Damage, Strain Localization and Size Effect, Elsevier, London, 1989, pp. 462–476.
[16] J. Planas, M. Elices, Nonlinear fracture of cohesive materials, Int. J. Fract. 51 (1991) 139–157.
[17] J. Planas, G.V. Guinea, M. Elices, Generalized size effect equation for quasibrittle materials, Fatigue Fract. Eng. Mater. Struct. 20 (5) (1997) 671–687.
[18] J. Planas, M. Elices, Shrinkage eigenstresses and structural size-effect, in: Z.P. Bazant (Ed.), Fracture Mechanics of Concrete Structures, Elsevier, London, 1992, pp. 939–950.